Journal of Thermal Analysis, Vol. 51 (1998) 49-62

PHASE BEHAVIOUR OF THE DIOCTADECYLDIMETHYL-AMMONIUM BROMIDE–WATER SYSTEM

P. C. Schulz[1*], *J. L. Rodríguez*[1], *F. A. Soltero-Martínez*[2], *J. E. Puig*[2] *and Z. E. Proverbio*[1]

[1]Departamento de Química e Ingeniería Química, Universidad Nacional del Sur, Bahía Blanca, Argentina
[2]Departamento de Ingeniería Química, Centro Universitario de Ciencias e Ingenierías, Universidad de Guadalajara, Guadalajara, Jelisco, México

Abstract

The phase behaviour of the twin-tailed surfactant dioctadecyldimethylammonium bromide with water was studied by DSC, FT-IR, X-ray and polarizing microscope. The phase diagram of DODAB–water system is very similar to that of DODAC–water. The dihydrate is in equilibrium with isotropic solution below 55°C. Above this temperature there is a lamellar liquid crystalline region, in equilibrium with isotropic liquid and solid crystals of DODAB·$2H_2O$, up to 69°C. From 69 to 86°C, the lamellar mesophase is in equilibrium with 'waxy' anhydrous DODAB. From 86 to 116°C and very high DODAB content, there is a very narrow region of existence of inverse hexagonal mesophase, in equilibrium via a narrow biphase region with lamellar mesophase. At $T>116$°C an isotropic liquid appears. There seems to exist two different lamellar mesophases, one of them between 10 and 40 wt.% DODAB and the other between 60 and about 97 wt.% DODAB, with a biphase zone between them.

Keywords: cationic surfactants, dioctadecyldimethylammonium bromide, mesophases, phase diagram, twin-tailed surfactants

Introduction

There is great interest in elucidating the phases which occur in systems of twin-tailed surfactants with water. The applications of these self-organized structures include processes as diverse as production of polymers with unusual structural and morphologycal characteristics [1], enhancement of analytical methods [2] and enhanced oil recovery [3].

Since twin-tailed surfactants are specially useful to produce model membranes and vesicles like biological membranes, which are used to investigate membrane-level processes in living beings, knowledge of the phase properties of this kind of surfactant is of great interest.

* Author to whom all correspondence should be addressed.

0368–4466/98/ $ 5.00

Akadémiai Kiadó, Budapest
Kluwer Academic Publishers, Dordrecht

The double-chained surfactant dioctadecyldimethylammonium bromide (DODAB) is a prototype for di-long-chain cationic surfactants salts. This compounds has been scarcely studied. Shorter homologues have been subject of studies in the past [4–7], and the chloride has been studied extensively in the last years [8–17].

Experimental

DODAB was purchased from Kodak and recrystallised. Water was double-distilled. Samples were prepared by direct addition of water to dried DODAB in sealed vials, then homogenized with sonication, maintained an hour at 100°C in a water bath and them allowed to equilibrate for at least a week at 25°C.

DSC curves were obtained with a Perkin-Elmer DSC-4 calorimeter. The instrument was calibrated with indium, water and *n*-octane standards. Cooling scans below room temperature were achieved with in Intracooler I refrigeration unit (Perkin-Elmer). All curves were determined with heating and cooling rates of $10°C\,min^{-1}$. Aluminium samples pans for volatile samples (Perkin-Elmer) were used to minimize losses by evaporation. Samples were weighed before and after DSC runs. Results with samples that lost weight were discarded. Transition temperatures were determined (±0.5°C) upon heating from the point at which the baseline changed slope significantly. Samples were normally cooled to temperatures of –50°C to ensure they were completely frozen.

Polarizing microscope observations were made in a Leitz crystallographic microscope with thermic plate and a digital temperature control.

Powder X-ray diffractograms were run in a Rigaku Denki diffractometer with a horizontal goniometer, CuK_α radiation, and a nickel filter. Wavelength was 0.15405 nm, goniometer rate $2°min^{-1}$, 35 kV, time constant 2 s, current intensity 12 mA, divergence slit 1°, reception slit 1°, and temperature 298 K. Diffractograms were indexed using the Vand method. (18,19) A Nicolet 5ZDA FT-IR spectrometer with a specially made electrically thermostatized cell was employed to run FT-IR spectra. CaF_2 windows were employed. Samples were sandwiched as thin films between the windows. The tension hydroxyl region ($3700–3100\,cm^{-1}$) was curve-fitted to three Gaussians with a curve fitting program (Peakfit) to study the structure of water.

Results

Figure 1 shows X-ray diffractogram of anhydrous DODAB at room temperature.

Figure 2 shows some representative DSC curves of the DODAB–water system.

Figure 3 shows melting enthalpy of water in the system, per gram of sample. It became zero at 97 wt.% DODAB. There was a break at 75 wt.% DODAB. As in some other systems [20, 21] extrapolation to 0 wt.% DODAB gave not the

melting enthalpy of pure water (320 J g^{-1}). In this system, the intercept gave ΔH_w°=400 J g^{-1}. Figure 3 also shows the melting enthalpy of the hydrocarbon chains, which became zero at 0 wt.% DODAB (whithin the experimental uncertainity). There was a break at 75 wt.% DODAB, with a reduction in the melting heat in samples of larger concentration.

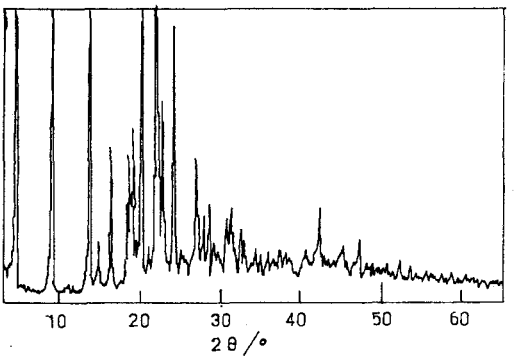

Fig. 1 X-ray diffractogram of anhydrous DODAB at room temperature

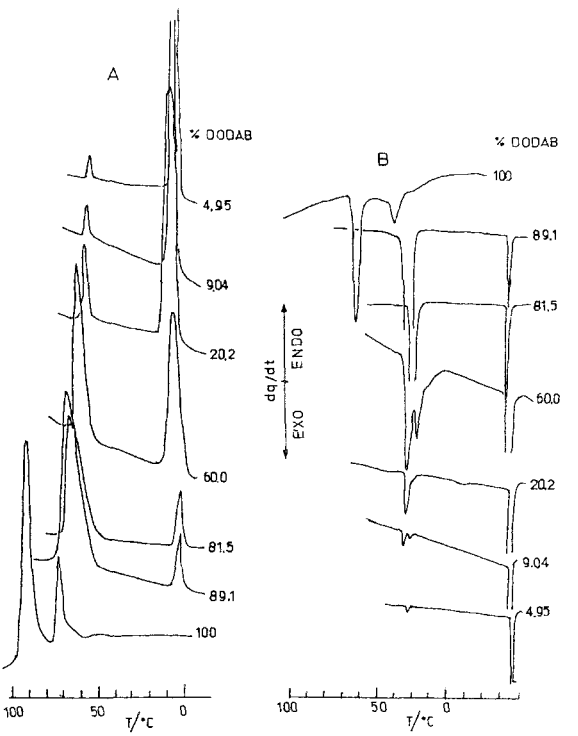

Fig. 2 Some representative DSC curves of the system DODAB–water

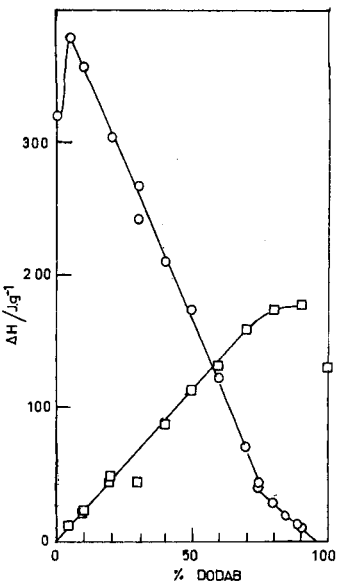

Fig. 3 Melting enthalpy of water (o) and surfactant chain (□) per gram of sample, *vs.* wt.% of DODAB

Table 1 Transition temperatures (°C)

% DODAB	Transition a	Transition b	Transition c	Transition d	Other
100					69a,b
					76a,b
					116a,b
95			71a,b	115.5a	
89.1	2a	54.5a	58a,b		
81.5	2a	54a	57a,b	115a	
70.48	2.5a	56a	56a		
60	3a	55a, 59b			
50	2a	55.5a, 56b			
40.2	1a	54a, 55b		109a	
30	2a	55a			
20.2	3a, 1a	53a, 55a, 55.5b			
9.04	1a, 3a	52a, 54a, 54.6b		100.2b	
4.95	0a, 1a	51a, 52a,b		99b	
0	0a				

[a]DSC determinations; [b]Polarizing microscope

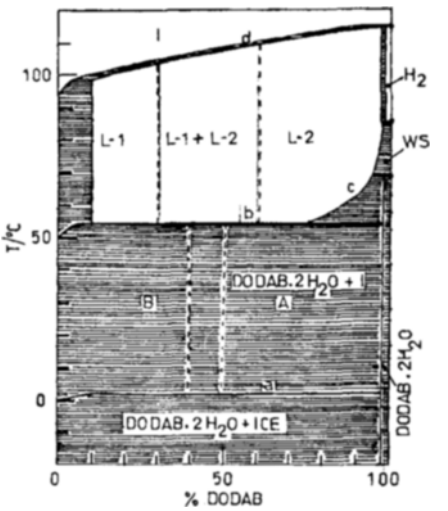

Fig. 4 Proposed phase diagram of DODAB–water system, a: water melting points, b: crystals to lamellar mesophase transition, c: border between mesophase and mesophase+solid biphase region, d: mesophase to isotropic liquid transition. L-1 and L-2: proposed two different lamellar mesophases. H-2: inverse hexagonal mesophase. WS: waxy solid, I: isotropic liquid, A: crystal paste, B: crystals immersed in continuous isotropic liquid

Table 1 shows the experimentally determined transition temperatures. Figure 4 shows the proposed phase diagram.

Discussion

X-ray determinations

The analysis of the X-ray diffractogram gave the structure of anhydrous DODAB. The unit cell was triclinic with a=1.0556±0.0081 nm, b=0.6896± 0.0053 nm, c=2.066±0.015 nm, α=101.86±0.79°, β=111.05 ±0.87°, γ=62.67± 0.43°. There were two molecules in the unit cell. The quantity (ab/2)sin β=0.3397±0.0027 nm^2 is taken as the cross section of the hydrocarbon chain, and is much higher than the common values obtained with other surfactant crystals: 0.1890 for lithium and cesium soaps [22, 23], 0.2094 for sodium soaps [24, 25], 0.182 for fatty acids [26, 27]. We made a DODAB molecule model with a computer program giving the molecule length l=2.71 nm from the center of the bromide ion and the middle point between the ends of the two tails. This value of l led us to suppose that the crystal surfactant palisade is monomolecular, because a biomolecular layer leads to an excesively low angle of tilt ($\tau \approx 21°$). The proposed structure is formed by an interdigitated packing, in whose {001} plane polar head groups alternate with terminal methyl groups. Similar interdigitated

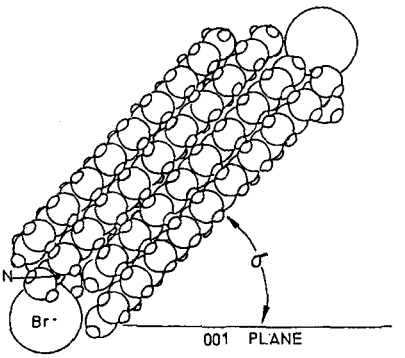

Fig. 5 Proposed packing of DODAB molecules in the elementary cell, viewed along the *b* axis. The σ angle between the {001} plane and the hydrocarbon tails zig-zag plane and the hydrocarbon tails zig-zag plane is also shown

structure was proposed by Klose *et al.* [28] for *n*-heptanephosphonic acid and *n*-octanephosphonic acid, and some surfactants of the N-alkanoyl-N-methylglucamie family also have interdigitated structures [29]. The proposed structure is that of Fig. 5, giving an effective molecule length of l_{eff}=2.97 nm. With l_{eff}= we computed the molecule total angle of tilt τ with respect to the {001} plane, which contains the polar layer, by:

$$\sin\tau = \frac{c\sin\beta}{l_{eff}} \tag{1}$$

giving τ=40.43±0.38°. This angle ranges from 49 to 55° for sodium alkanephosphonatetτs [3]. For another twin-tailed surfactant, sodium di-octylphosphinate, τ=47.63±0.39° [31]. The value of τ is 53° for potassium soaps [32]. This tilt is composed by two different angles [31]: one of 60° between the chain and the {001} plane in the plane of the chains zig-zag, imposed by the all-trans conformation of the hydrocarbon chains. This angle of 60° may be seen by looking at the molecules along the *a* axis (Fig. 6). The other angle σ is the tilt of the zig-zag plane with respect to the {001} plane. It may be seen by looking at the molecule along the *b* axis (Fig. 5), and is given by [31]:

$$\sin\sigma = \frac{c\sin\beta}{2l\sin 60} \tag{2}$$

giving σ=48.49±0.49°. The value of ε=$b/(a \sin\beta)$=0.7000±0.0051 is taken as the d_1/d_2 ratio, where d_2 is the width of the molecule in the zig-zag plane and d_1 the width of the molecule normal to this plane. This value is similar to that obtained in other surfactant crystals: 0.6410±0.0020 for *n*-alkanephosphonates [30], 0.66 for sodium palmitate [24, 25], 0.62 for some fatty acids [27], 0.701±0.035 for so-

dium dioctylphosphinate [31]. The surface per polar head in the plane {001} was S=0.3233±0.0025 nm^2. It is larger than the values for single-chained surfactants: 0.27358±0.00033 for sodium *n*-alkane phosphonates [30], 0.1890 for lithium and cesium soaps at 25°C [22, 23], but is similar to that of other twin-chained surfactant, sodium dioctylphosphinate, which showed S=0.30366±0.00034 nm^2 [31]. The presence of the bulky bromide ion may contribute to the increase of S. Notice that the model of interdigitated monomolecular crystalline layers leads to a cross section of the hydrocarbon chain value of (ab/4)sin β=0.1699± 0.0027 nm^2, a more normal value. The molar volume of surfactant was 375.5±1.7 cm^3 mol^{-1}, and the crystallographic density was δ=1.6057±0.0073 g cm^{-3}.

DSC measurements

The hydrocarbon chains of anhydrous DODAB melted at 60.0 and 69.0°C with an enthalpy of 50 J g^{-1}. There is gradual reduction of this temperature when water is added to the system, and reaches an almost constant value of 55°C at 75 wt.% DODAB. The hydrocarbon chains peak is composed by two very close peaks. In heating curves, one of them appeared as a shoulder in the other peak. They are specially visible in the cooling curves, and sometimes the separation is well visible as in the 60.0 and 9.04 wt.% samples in Fig. 2. The ratio between the largest and the smallest peak areas is 1.7±0.3. This phenomenon probably means that the two chains are not equivalent. On the supposition that each peak corresponds to the melt of one of the chains, one of them melts first with an enthalpy of 31 J g^{-1} of sample, and the other with an enthalpy of 19 J g^{-1} of sample in pure DODAB. This means that the first chain melts with an enthalpy of 77 J g^{-1} of chain, and the other with 47 J g^{-1} of chain. The melting enthalpy of octadecane is 241 J g^{-1}, and its melting point is 28.2°C [33]. The melting point of the surfactant chains is higher because of the extra cohesion given by the ionic layer. According to the Kirchhoff law, an increase in the melting temperature must cause a reduction in the melting enthalpy, as it was observed. The fusion of the first chain reduces the cohesion of the second one, which melts with lower enthalpy. The introduction of water weakens the ionic layer, and the melting point of the chains decreases. In Fig. 3 it may be seen that there is a change in the dependence of the melting enthalpy at about 75 wt.% DODAB. At this concentration, the melting peak of the polar network disappeared, whilst between 75 and 97% the peaks of the chains and the polar heads are overlapping (that of hydrocarbon network fusion appears as a shoulder in the polar network fusion). This means that the enthalpy points in this range are the sum of chain and polar head fusion.

In pure DODAB, the polar layer melted at 86.5°C, with an enthalpy of 130 J g^{-1}. At 120°C another transition appeared.

The melting point of water was 0°C at low concentrations (0 to ~10 wt.% DODAB) and about 2°C at all other concentrations at which the water melt was detected. The melting enthalpy of water became zero at 97 wt.% DODAB, which corresponds to two water molecules per surfactant molecule (Fig. 3). This dihy-

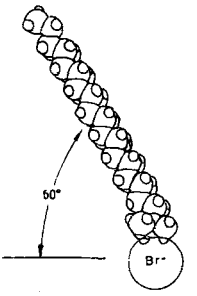

Fig. 6 Molecule in the crystal, viewed along the *a* axis, showing the 60° angle due to the zig-zag conformation

drate was also found in didodecyldimethylammonium bromide [34] and in dioctadecydimethylammonium chloride [8].

The change in slope at 75 wt.% DODAB indicates that there is a change in properties of 'free' water at this concentration, which coincides with the disappearance of the melting peak of the polar heads. This concentration corresponds to 11.7 water molecules per surfactant molecule. Two water molecules may be attributed to the bromide ion hydration, the other 9.7 may be due to the formation of a hydrophobic hydration shell around the dimethylammonium ion. At DODAB concentrations lower than 75%, the melt of the chains causes the solubilisation of the polar heads and the destruction of the crystalline structure of the polar network.

Polarizing microscope observations

Observation with the polarizing microscope showed that in pure DODAB, the fusion of the hydrocarbon tails did not change the external shape of crystals, but its texture between crossed polarizers became turbid, in contrast with the transparent texture of low temperature crystals. We named this texture 'waxy solid' (Fig. 7). If the melting point of the polar network was not reached, this phenomenon was reverted while cooling. The melt of the polar network produced a fluid liquid. This liquid was pseudoisotropic. With vigorous motion between slides the liquid gave a cloudy texture. This texture was the non-geometric of hexagonal mesophases, and must correspond to an inverse (H_2) phase. The domain of existence of this inverse hexagonal mesophase is very narrow. It must be noted that in DODAB–water system, Laghlin *et al.* [8] did not found any inverse hexagonal mesophase. The transition point at 120°C corresponds to the formation of an isotropic liquid. On cooling the fused pure DODAB, a very strange texture was obtained (Fig. 8). On a slightly cloudy, scarcely birrefringent background, many strongly birrefringent, golden structures appeared, with shape of twin needles. The macroscopic aspect is a transparent, colourless solid. This texture did not appear if water was present in the sample.

At curve b, crystals start to form lamellar liquid crystals, showing a network of golden oily streaks on a pseudoisotropic background (Fig. 9) and positive and negative units. In some cases, terraced textures also appeared. At concentrations lower than 10%, myelin-like textures and positive spherulites appeared on an isotropic background. At concentrations lower than 10 wt.% DODAB, isotropic liquid appeared in equilibrium with mesomorphic textures.

If the samples were not homogenized by fusion at the boiling water bath, the melt of the crystals started at about 70°C. These samples were in a nonequili-

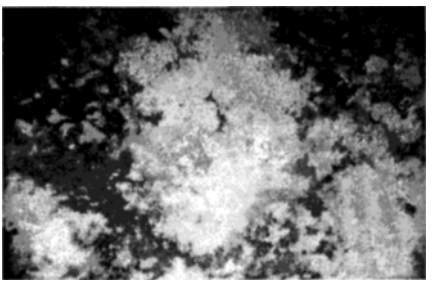

Fig. 7 Waxy crystals of 100% DODAB at 72°C, crossed polaroids, ×100

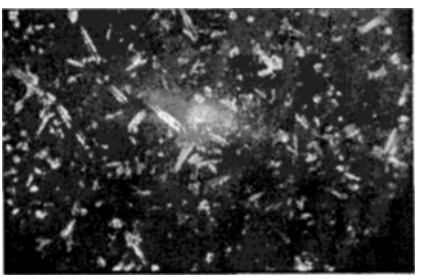

Fig. 8 Anhydrous solid DODAB after melting and cooling. Crossed polaroids, ×100

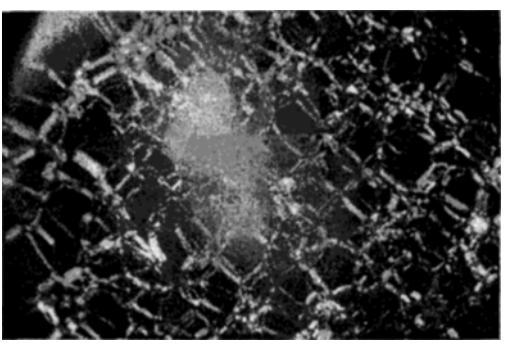

Fig. 9 Oily streacks, 40 wt.% DODAB at 74.5°C, crossed polaroids, ×100

brium starting state, because by contact of anhydrous crystals and water at room temperature, the equilibrium was reached very slow. Laughlin *et al.* [8] reported that it took a mounth to form DODAC dihydrate.

FT-IR determinations

The FT-IR determinations were performed at two different temperatures: 20°C, where crystals exist and at 60°C at which liquid crystals exist. At high DODAB concentrations the $\nu_a(CH_3-)$ peak produced an interference. The $\nu_a(CH_3-)$ peak appeared at 2950.6±1.4 cm^{-1} with σ=109±81 at 20°C and 2977.0±1.9 cm^{-1} with σ=108±45 at 60°C.

At 20°C the systems were composed by crystals and isotropic solution. There were three different types of water [35–38]: bulk-like, 'interfacial' and 'trapped'

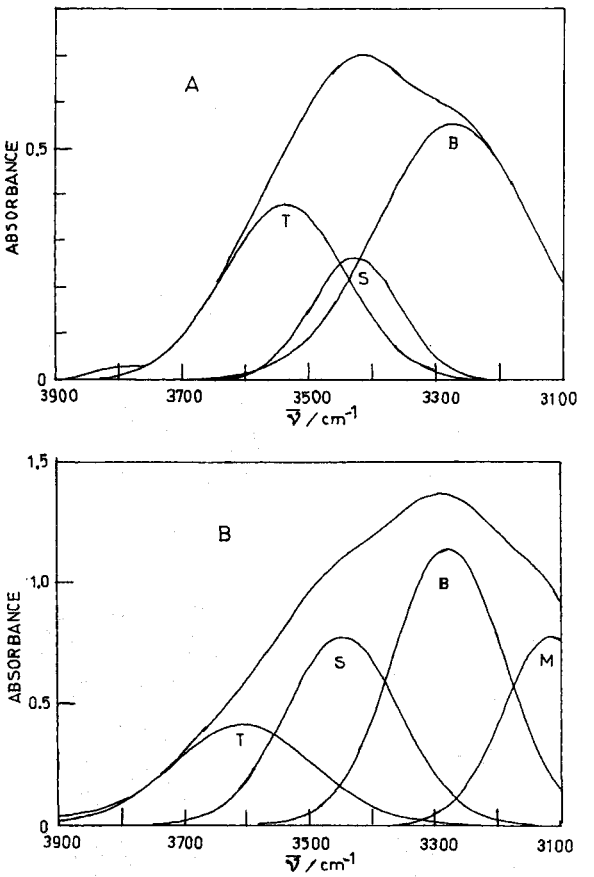

Fig. 10 Deconvolution of the water ν_{OH} band: B – bulk like water, S – surface water, T – trapped water, M – ν_a methyl peak. a) 20 wt.% DODAB 20°C, without methyl interference; b) 40 wt.% DODAB 60°C, with methyl group interference

water. The three peaks fitted to Gaussians with the following parameters: μ_B=3314±22 cm^{-1} (σ=108±45) (bulk-like), μ_s=3432.6±5.5 cm^{-1} (σ=90±46) (interfacial) and μ_T=3532±12 cm^{-1} (σ=77±22) (trapped). As an example, in Fig. 10 it may be seen the deconvolution of one ν_{OH} peak with ν_{CH_3} interference and other peak without interference.

Bulk-like or 'free' water is assumed to have physicochemical properties not much different from those of pure water. Interfacial water was also named 'solvent shell' [39] or 'vicinal water' [40]. This water may be defined as water molecules which had been influenced by the surface of the substrate in contact with water [41]. Trapped water are isolated water molecules in the surfactant structure matrix.

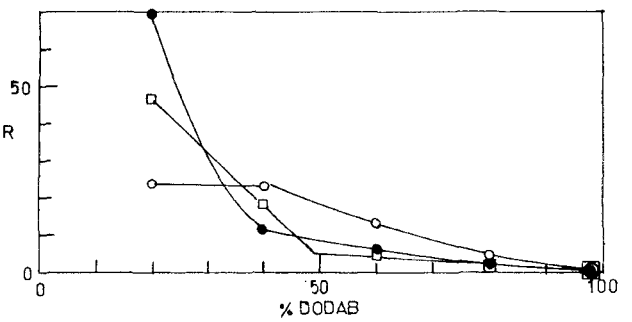

Fig. 11 Moles of water per surfactant molecule •: R_B, o: R_S, □: R_T at 20°C

In Fig. 11 we show the number of water molecules of each type per surfactant molecule in the system, R_B, R_S and R_T, *vs.*the total DODAB wt.% at 20°C. It may be seen that bulk-like water (R_B) increased very slowly with increasing water concentration up to about 60% water (40 wt.% DODAB), and then R_B rose speedly. Surface water (R_S) increased with water concentration up to ~60% water, and then reached a plateau. Trapped water increased slowly up to ~51% water and then increased more speedly. Microscopic observations showed that up to about 60% water, a white paste formed by crystals could be seen. All water, including 'free' water, is placed in the crystals pores and surface. At water contents >60%, the crystals could be seen immersed in isotropic solution. We concluded that up to ~60% water, any water addition goes to the crystal pores and surface producing an increase in the crystal/solution interfase. At ~51% water, the crystal matrix is open enough to provide new small loci to the trapped molecules. These probably are imperfections in the polar layers exposed to the aqueous solution. At water content >60%, the total interface crystal/solution per surfactant molecule remained constant and any water addition gave mainly free water.

At 60°C liquid crystals exist. The parameters of the Gaussians were μ_B=3211.5±7.5 cm^{-1} (σ=79±29) (bulk-like), μ_S=3400±12 cm^{-1} (σ=89±20) (interfacial) and μ_T=3564±39 cm^{-1} (σ=94±25) (trapped). The different types of

water are shown in Fig. 12. Free water was almost constant up to 60 wt.% water ($R_B \approx 2.5$), and then rose to about $R_B=20$. Surface water increased slowly up to 20% water ($R_S \approx 4$), in the biphase region, then rose to $R_S \approx 18$ at 40% water, remained constant up to 60% water and then rose again. Trapped water remained almost constant ($R_T \approx 2$) up to 40 wt.% water, and then rose monotonically. In other mesophase systems, these changes in behaviour were detected at regions in which changes in the liquid crystal structure were detected. Since in the whole region only typical lamellar mesophase textures were seen, we conclude that there may be a change in the lamellar phase structure, as it has been detected in didodecyldimethylammonium bromide–water systems [42]. We named the two possible lamellar mesophases as *L*-1 and *L*-2.

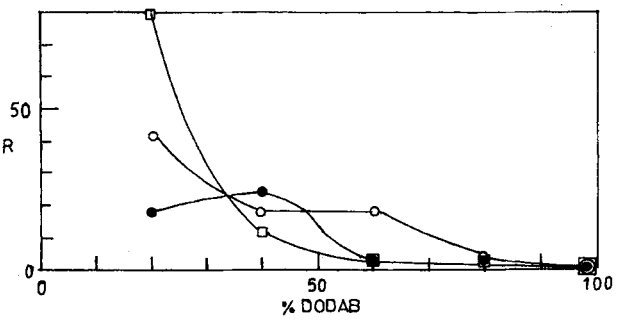

Fig. 12 Moles of water per surfactant molecule •: R_B, o: R_S, □: R_T at 60°C

The reduction of bulk water in changing from crystal+isotropic solution to liquid crystals is not surprising, because the ionic bilayer was destroyed and all the polar headgroups became exposed to the aqueous solution. The exception at 40% DODAB was probably due to the very high interference of the methyl peak, which increased the uncertainty of the area measurement of the bulk-like water. The amount of surface water increased, as it might be expected. On increasing water content, the average distance among polar headgroups in the polar bilayer surface increased, giving an increased interface to interact with surface water, and more interstices to locate trapped water.

In anionic surfactant systems, surface water can be detected by DSC measurements and up to three different types were detected in different systems [30, 38, 43]. As it might be seen in this work, surface water also exist in the DODAB–water system, and it was detected by FT-IR in other cationic surfactant–water system, dodecylallyldimethylammonium bromide [44]. However, it might not be detected by DSC. It implies that the interaction between water and cationic interfaces is different from that with anionic interphases. The cationic interface–water interaction can be weak enough to allow the surface water to melt at temperatures close enough to that of pure water to be undetectable by DSC. Hydrophobic hydration is known to give stronger hydrogen-bonding, which may explain the melting of water at about 2°C in concentrated samples.

Conclusions

The phase diagram of DODAB–water system is very similar to that of DODAC–water.

Below 55°C there are crystals and isotropic solution. Crystals in equilibrium with water are DODAB·$2H_2O$. Between about 50 wt.% DODAB and DODAB·$2H_2O$, water is included in pores and surfaces, and the increase of water content increases the interphase crystal-water. At concentrations below 40 wt.% DODAB, crystals are immersed in a continuous isotropic solution.

At T>55°C, there is a lamellar liquid crystalline region. The low-concentration border about 10 wt.% DODAB, in which there is a biphase region of coexistence of lamellar mesophase and isotropic liquid. The high-concentration border is a biphase region of coexistence of lamellar mesophase and solid DODAB·$2H_2O$, up to 69°C. From 69 to 86°C, the biphase region corresponds to lamellar mesophase and 'waxy' anhydrous DODAB. From 86 to 116°C, there are a very narrow region of existence of inverse hexagonal mesophase, in equilibrium via a narrow biphase region with lamellar mesophase. At T>116°C an isotropic liquid appears.

There seems to exist two different lamellar mesophases, one of them between 10 and 40 wt.% DODAB and the other between 60 and 97 wt.% DODAB, with a biphase zone between them.

At very low concentrations, the lamellar mesophase disappears at about 100°C.

* * *

One of us (JLR) has a fellowship from the Comisión de Investigaciones Científicas de la Provincia de Buenos Aires. This research was partially supported by a grant of the Comisión de Investigaciones Científicas de la Provincia de Buenos Aires, and partially by a grant of the Universidad Nacional del Sur.

References

1 J. E. Puig., S. Corona-Galván, AS. Maldonado, P. C. Schulz, B. Rodríguez and E. W. Kaler, J. Colloid Interface Sci., 137 (1990) 308.
2 P. C. Schulz, B. S. Fernández-Brand, M. Palomeque and A. L. Allan, Colloids Surf., 49 (1990) 321.
3 M. Latil, Enhanced Oil Recovery; Gulf Publishing Co., Houston TX, 1980.
4 T. Kunitake, Y. Okahata, K. Tamaki, F. Kamamaru and M. Takayanagi, Chem. Lett., (1977) 387.
5 A. Kumano, T. Kajiyama, M. Takayanagi, T. Kunitake and Y. Okahata, Ber. Bunsen-Ges. Phys. Chem., 88 (1984) 1216.
6 E. Z. Radlinska, T. Z. Zemb, J.-P. Dalbiez and B. W. Ninham, Langmuir, 9 (1993) 2844.
7 T. Kajiyama, A. Kumano, M. Takayanagi, Y. Okahata and T. Kunitake, Contemp. Top. Polym. Sci., 4 (1984) 829.
8 R. G. Laughlin, R. L. Munyon, Y.-C. Fu and A. J. Fehl, J. Phys. Chem., 94 (1990) 2546.
9 T. Imae, T. Tsubota, H. Okamura, O. Mori, K. Takagi, M. Itoh and Y. Sawaki, J. Phys. Chem., 99 (1995) 6046.

10 R. G. Laughlin, R. I. Munyon, Y.-C. Fu and T. J. Emge, J. Phys. Chem., 95 (1991) 3852.
11 R. G. Laughlin, R. I. Munyon, J. L. Burns, T. W. Coffindaffer and Y. Talmon, J. Phys. Chem., 96 (1992) 374.
12 A. M. Carmona-Ribeiro, J. Phys. Chem., 97 (1993) 11843.
13 K. Deguchi and J. Mino, J. Colloid Interface Sci., 65 (1978) 155.
14 A. M. Carmona-Ribeiro, J. Phys. Chem., 93 (1989) 2630.
15 E. A. Lissi, S. Gallardo and P. Sepúlveda, J. Colloid Interface Sci., 152 (1992) 104.
16 H. J. Watzke and J. H. Fendler, J. Phys. Chem., 91 (1987) 854.
17 T. Kawai, J. Umemura and T. Takenaka, Langmuir, 2 (1986) 739.
18 V. Vand, Acta Crystallogr., 1 (1948) 109.
19 V. Vand, Acta Crystallogr., 1 (1948) 290.
20 K. P. Antonsen and A. S. Hoffman in Poly(ethylene glycol) Chemistry, Biotechnical and Biomedical Applications, J. M. Harris, Ed., Plenum Press, New York 1992, p. 15.
21 T. de Vringer, J. G. H. Joosten and H. E. Juninger, Colloid Polym. Sci., 264 (1986) 263.
22 B. Gallot and A. E. Skoulios, Kolloid Z., 209 (1966) 164.
23 B. Gallot and A. E. Skoulios, Kolloid Z., 213 (1968) 143.
24 J. W. McBain, O. E. A. Bolduan and S. Ross, J. Am. Chem. Soc. 65 (1941) 1873.
25 J. W. McBain, A. de Bretteville and S. Ross, J. Chem. Phys. 11 (1943) 179.
26 R. Brill and K. H. Meyer, Z. Krist. 67 (1928) 570.
27 A. Muller, Proc. Roy. Soc. (London) 114A (1927) 542.
28 G. Klose, A. G. Petrov, F. Volk, H. W. Mayer, G. Förster and W. Rettig, Mol. Cryst. Liq. Cryst. 88 (1982) 109.
29 G. A. Jeffrey and H. Maluszynka, Acta Cryst. B45 (1989) 447.
30 P. C. Schulz, Anales Asoc. Quím. Argentina, 71 (1983) 271.
31 P. C. Schulz and J. E. Puig, Langmuir 8 (1992) 2623.
32 T. R. Lomer, Acta Cryst. 5 (1952) 11.
33 Handbook of Chemistry and Physics, The Chemical Rubber Co, Cleveland 1970.
34 P. C. Schulz, J. E. Puig, G. Barreiro and L. A. Torres, Thermochim. Acta, 231 (1994) 239.
35 T. K. Jain, M. Varshney and A. Maitra, J. Phys. Chem., 93 (1989) 7409.
36 T. L. Tso and E. K. C. Lee, J. Phys. Chem., 89 (1985) 1612.
37 G. E. Walfraen, in A. K. Covington and P. Jones, eds. Hydrogen Bonded Solvent Systems, Taylor and Francis, London 1968.
38 J. E. Puig, J. F. A. Soltero, E. I. Franses, L. A. Torres and P. C. Schulz, in A. K. Chattopdhyay y K. L. Mittal, eds. 'Surfactants in Solution' Marcel Dekker, New York 1996, p. 147.
39 J. A. Rupley and G. Careri, Adv. Protein Chem., 41 (1991) 37.
40 G. Wilse Robinson and S. B. Zhu, in J. Jormer et al., eds, Reaction Dynamics in Clusters and Condensed Phases, Kluwer Academic Publishers, Dordrecht 1994, p. 423.
41 N. Garti, A. Aserin, S. Ezrahi, I. Tiunova and G. Berkovic, J. Colloid Interface Sci., 178 (1996) 60.
42 K. Fontell, A. Ceglie, B. Lindman, B. Ninham, Acta Chem. Scand. A40 (1986) 247.
43 N. Casillas, I. Rodríguez-Siordia, V. M. González-Romero and J. E. Puig, in Memorias del XIII Congreso de la Academia Nacional de Ingenieria, México (1987).
44 P. C. Schulz, unpublished results.